Pairing correlations in electron-doped cuprates

A. A. Aligia[1] and Liliana Arrachea[2]
[1]*Centro Atómico Bariloche and Instituto Balseiro, Comisión Nacional de Energía Atómica, 8400 Bariloche, Argentina*
[2]*Departamento de Física, FCEyN Universidad de Buenos Aires, Pabellón I, Ciudad Universitaria, 1428 Buenos Aires, Argentina*
(Received 3 June 2001; published 13 November 2001)

We calculate on-site *s*, extended *s* and $d_{x^2-y^2}$ pairing correlation functions in a generalized Hubbard model for the cuprates, for parameters appropriate for electron-doped systems, using numerical diagonalization of a 4×4 cluster. We find indications of *d*-wave superconductivity for small doping (~0.1 electrons per unit cell) and *s*-wave superconductivity for overdoped systems (~0.5 electrons per unit cell) or small *U*. The magnitude of the pairing correlation functions and the vertex contributions to them are in general much smaller than in the hole-doped case. We also present results for the spin-structure factor.

DOI: 10.1103/PhysRevB.64.214518 PACS number(s): 74.20.−z, 71.27.+a

I. INTRODUCTION

The origin of the pairing mechanism and the symmetry of the order parameter in electron-doped cuprate superconductors, such as $Nd_{1-x}Ce_xCuO_4$ (NCCO) or $Pr_{1-x}Ce_xCuO_4$ (PCCO) remains controversial. Tunneling experiments[1] indicate the presence of at least some *s*-wave components in the superconducting gap, and Raman measurements are consistent with a nearly uniformly gapped Fermi surface.[2] Microwave-penetration-depth experiments in NCCO were considered as evidence for *s*-wave pairing,[3] but a recent reinterpretation of similar experiments suggests a strongly anisotropic gap in both NCCO and PCCO.[4] Also, phase-sensitive experiments in tricrystal films suggest that the order parameter has a large component with $d_{x^2-y^2}$ symmetry,[5] which is in agreement with photoemission experiments.[6] An important part of the experimental evidence might be rendered consistent if the order parameter contains both *s* and $d_{x^2-y^2}$ components. On the theoretical side, this feature is obtained in a generalized *t*-*J* model[7,8] where the ground state has a significant overlap with a resonance-valence-bond wave function.[8] However, an analysis based on a Ginzburg-Landau theory indicates that a mixed order parameter would require two phase transitions as the temperature is increased.[9]

While the experimental situation is still not settled, it is important to clarify if any realistic effective model for the electron cuprates can lead to nonconventional *s*-wave superconductivity or not. The electron-phonon interaction usually gives rise to an *s*-wave superconducting gap, but it is not expected to lead to T_c of the order of 20 K in systems with a comparatively low density of states and number of carriers. Conventional superconductivity with $T_c=39.5$ K, has been recently found in MgB_2.[10] However, this compound is markedly different from the cuprates since there is a strong coupling with high-frequency phonon modes and a very small Coulomb repulsion.[11] Theoretically, it has been proposed that electron-phonon interaction can lead to high T_c in the cuprates, even with $d_{x^2-y^2}$ symmetry[12] if the Fermi level is near a van Hove singularity of the two-dimensional band structure (leading to a high density of states at the Fermi level). As discussed below, this is clearly not the case of electron-doped cuprates.

In principle, one could expect that the *t*-*J* model including next-nearest-neighbor hopping t' is the appropriate model to describe electron-doped superconductors[13,14] (see the Appendix). It is known that this model leads to $d_{x^2-y^2}$-wave superconductivity. To our knowledge, a similar model leading to *s*-wave superconductivity has not been derived. One possibility in this direction is to consider excitonic pairing mechanisms[15,16] that have been proposed in the search for a common pairing mechanism in all perovskite superconductors, including doped $BaBiO_3$.[17] However, the results of Ref. 15 might be an artifact of the particular form chosen for the distance dependence of interatomic repulsions. An effective attraction between electrons added in next-nearest-neighbor positions, driven by nearest-neighbor Cu-O repulsion, has been obtained using perturbation theory.[16] However, a numerical study of the appropriate generalized *t*-*J* model that contains this interaction, indicates that this term does not lead to superconductivity.[18] The derivation of this effective model is described in the Appendix.

Another effective model for the cuprates in which double occupancy at each effective Cu site is allowed is the Hubbard model with nearest-neighbor correlated hopping and next-nearest-neighbor hopping t'.[19–21] Since the effective on-site repulsion *U* in this model is related to the Cu-O charge-transfer energy Δ,[20] and this energy is lower in electron-doped cuprates due to the absence of apical O atoms,[22] it seems particularly important here to consider a finite *U*. In addition, a finite *U* enhances the mobility of superconducting pairs.[23,24] The superconductivity in this model was studied previously within a Hartree-Fock Bardeen-Cooper-Schrieffer (BCS) approximation.[25,26] If $t'=0$, only *s*-wave superconductivity for high-enough doping is obtained.[25] However, for the hole-doped system with realistic or large t', $d_{x^2-y^2}$-wave superconductivity takes place at dopings for which the Fermi level is near the van Hove singularity, if the correlated hopping is large enough to overcome the antiferromagnetic instability.[26] Furthermore, the $d_{x^2-y^2}$-wave superconductivity survives if the effect of short-range antiferromagnetic spin fluctuations is included.[26] This picture suggests that if the system is doped with electrons instead of holes, the Fermi surface moves away from the van Hove singularities and the dominant superconducting instability would have *s*-wave symmetry. This is an interesting situation; the same

model would lead to $d_{x^2-y^2}$-wave superconductivity for doping with holes and to *s*-wave superconductivity for electron doping. The case of hole doping has received strong support by our recent numerical studies on a cluster containing 4 $\times 4$ unit cells.[27] This was the first report on pairing correlation functions in any generalized Hubbard model and required a big computational effort and the use of group theory to reduce the size of the matrices by a factor 256.

This work extends the numerical study to the case of the electron-doped system, keeping the same parameters that led to $d_{x^2-y^2}$-wave superconductivity in the hole-doped case. In Sec. II we briefly describe the model. Section III contains a few technical explanations and the results for the pairing correlation functions, their vertex contributions, and spin-spin correlation functions for different electron dopings. Section IV contains a summary and a brief discussion.

II. THE EFFECTIVE MODEL

The effective model we consider was derived from the three-band model for the cuprates H_{3b} [Eq. (A1)],[28] through the following steps:[19–21] (i) change the basis of the $2p_\sigma$ O orbitals to Wannier functions α_i, γ_i centered at each Cu site i (the former has x^2-y^2 symmetry, such as the relevant Cu $3d$ orbital d_i), (ii) solve H_{3b} neglecting intersite terms in this basis, (iii) map the states of lowest energy for each effective site i with 0, 1, and 2 holes, into the corresponding states of the Hubbard model, and (iv) calculate the intersite terms in this restricted basis, including other states perturbatively. The resulting one-band Hamiltonian that describes the motion of *holes* in electron-doped systems has the form

$$H=U\sum_i n_{i\uparrow}n_{i\downarrow}-t'\sum_{\langle ij'\rangle\sigma}c^\dagger_{i\sigma}c_{j'\sigma}-\sum_{\langle ij\rangle\sigma}(c^\dagger_{i\sigma}c_{j\sigma}+\text{H.c})\times\{t_{AA}(1-n_{i\sigma})(1-n_{j\sigma})+t_{BB}n_{i\sigma}n_{j\sigma}+t_{AB}[n_{i\sigma}(1-n_{j\sigma})+n_{j\sigma}(1-n_{i\sigma})]\}, \quad (1)$$

where $\langle ij\rangle$ ($\langle ij'\rangle$) denotes nearest-neighbor (next-nearest-neighbor) positions of the lattice. Here the vacuum state corresponds to the $3d^{10}$ configuration of Cu and $2p^6$ configuration of each O atom. The state $c^\dagger_{i\sigma}|0\rangle$ represents the ground state of H_{3b} within site i with one hole and has the form $(Ad^\dagger_{i\sigma}+B\alpha^\dagger_{i\sigma})|0\rangle$. Similarly $c^\dagger_{i\uparrow}c^\dagger_{i\downarrow}|0\rangle$ represents the ground state with two holes at effective site *i*, which has the form of a Zhang-Rice singlet, $[A(\alpha^\dagger_{i\uparrow}d^\dagger_{i\downarrow}-\alpha^\dagger_{i\uparrow}d^\dagger_{i\downarrow})+Bd^\dagger_{i\uparrow}d^\dagger_{i\downarrow}+C\alpha^\dagger_{i\uparrow}\alpha^\dagger_{i\downarrow}]|0\rangle$.

The Hamiltonian is the same as that used before by us for hole doping.[26,27] However, in the representation used here $c^\dagger_{i\sigma}$ creates holes (instead of electrons) so that t_{AA} and t_{BB} are interchanged and t' is *positive* (a change of sign of all nearest-neighbor hopping does not affect the physics in a bipartite lattice). The hopping parameter t_{AB} is expected to be larger than $(t_{AA}+t_{BB})/2$.[19,20] This is clearly the case for small Cu-O hopping t_{pd}.[25] As in previous studies we take $t_{AA}=t_{BB}=1$ as the unit of energy and choose somewhat exaggerated values of t_{AB} in order to enhance the superconducting signals. We also retain the value $t'=0.45$ (Refs. 14 and 29) used for the hole-doped case (with opposite sign due to the electron-hole transformation).

III. NUMERICAL METHOD AND RESULTS

In this section, we present results for the pairing correlation functions as functions of distance, and the spin-structure factor as a function of wave vector, for different occupations, in a square lattice containing 16 unit cells. The calculations were done using the Lanczos method.[30] The size of the Hilbert space and the number of nonzero matrix elements after inclusion of next-nearest-neighbor hopping, is near the limit of present state of the art numerical diagonalizations. To render the computation feasible, we have exploited all symmetry operations of the space group of the square lattice[31] plus time reversal and total spin projection. For each number of holes N (corresponding to electron doping $x=1-N/16$), we have calculated the correlation functions for two values of t_{AB} (1 and 2) and three values of U (0, 4, and 10), keeping $t_{AA}=t_{BB}=1$ and $t'=0.45$.

In each case we have first verified which are the optimum boundary conditions (OBC) for the set of parameters chosen. We define the OBC as the boundary conditions (BC) leading to the minimum ground-state energy. The different BC considered are as follows: periodic in both directions (PBC), antiperiodic in both directions (ABC), or mixed (MBC). For the noninteracting system ($U=0$), it is known that the use of twisted boundary conditions allows one to represent all wave vectors even if one is working with a finite system. Minimizing with respect to the boundary conditions leads then to the best possible representation of the filled Fermi sea in the thermodynamic limit and usually to a nondegenerate closed-shell configuration for the ground state. In one dimension, it has been verified that the choice of OBC leads to a smoother variation of several quantities as the size of the system is increased, alternating PBC and ABC.[32] In our system, OBC ensure closed-shell configurations for the noninteracting system ($U=0$) in most of the fillings under consideration, with the only exception of the case with $N=14$. In a previous work,[33] it was verified that the occupation in k space is mildly modified as the interaction U is switched on and that OBC lead to a nondegenerate closed-shell ground state with total spin $S=0$. Thus, we assume that these OBC most reliably represent the physical behavior of the system in the thermodynamic limit and use them in the rest of the computations.

To save memory, the operators that entered the different calculations were symmetrized with respect to the point-group operations. This is a technical trick that does not affect the results.

The pairing correlation functions are defined as

$$P_\alpha(i)=\langle\Delta^\dagger_\alpha(i)\Delta_\alpha(0)\rangle, \quad (2)$$

where for on-site *s* pairing $\Delta^\dagger_{os}(i)=c^\dagger_{i\uparrow}c^\dagger_{i\downarrow}$, while $\Delta^\dagger_\alpha(i)=\Sigma_\delta f_\alpha(\delta)(c^\dagger_{i+\delta\uparrow}c^\dagger_{i\downarrow}-c^\dagger_{i+\delta\downarrow}c^\dagger_{i\uparrow})/\sqrt{8}$, with $f_{es}(\delta)=1$ for extended *s* pairing and $f_d(\delta)=1$ [$f_d(\delta)=-1$] when $\delta=\pm(1,0)$ [$\delta=\pm(0,1)$] for $d_{x^2-y^2}$ pairing. We normalize $\Delta^\dagger_\alpha(i)$ in such a way that $|\Delta^\dagger_\alpha(i)|0\rangle|^2=1$, to facilitate com-

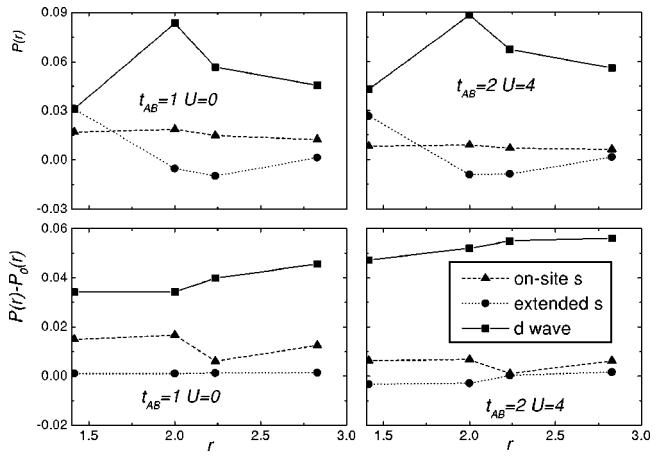

FIG. 1. Pairing correlation functions $P_\alpha(r)$ (top) and vertex contributions $\overline{P}_\alpha(r)$ (bottom) as functions of distance for $N=14$ and different parameters (left: $t_{AB}=1$, $U=0$, right: $t_{AB}=2$, $U=4$). Triangles, circles, and squares correspond to on-site s, extended s and $d_{x^2-y^2}$ symmetry, respectively.

parison among the different pairing correlation functions. We also compute the so-called vertex contribution to the pairing correlation functions,[34] denoted as $\overline{P}_\alpha(i)$. In order to do this, the quantity $(\langle c_\lambda^\dagger c_\xi\rangle\langle c_\mu^\dagger c_\nu\rangle-\langle c_\lambda^\dagger c_\nu\rangle\langle c_\mu^\dagger c_\xi\rangle)$ is subtracted, for every term in Eq. (2) of the form $\langle c_\lambda^\dagger c_\mu^\dagger c_\nu c_\xi\rangle$. The importance of the vertex contributions resides in that for a BCS ground state, $\overline{P}_\alpha(i)$ is positive and proportional to the square of the order parameter. Then, one can expect that they represent a more sensitive measure of superconductivity, and that part of the finite-size effects is canceled in the substraction. For MBC there are two nonequivalent lattice vectors at some distances and the reported pairing correlation functions are averages over all lattice vectors with the same modulus. Following our previous experience,[27] we will assume that superconducting correlations in the α channel are present in the model when *both quantities*, P_α and $\overline{P}_\alpha$, are enhanced at large distances relative to the noninteracting case.

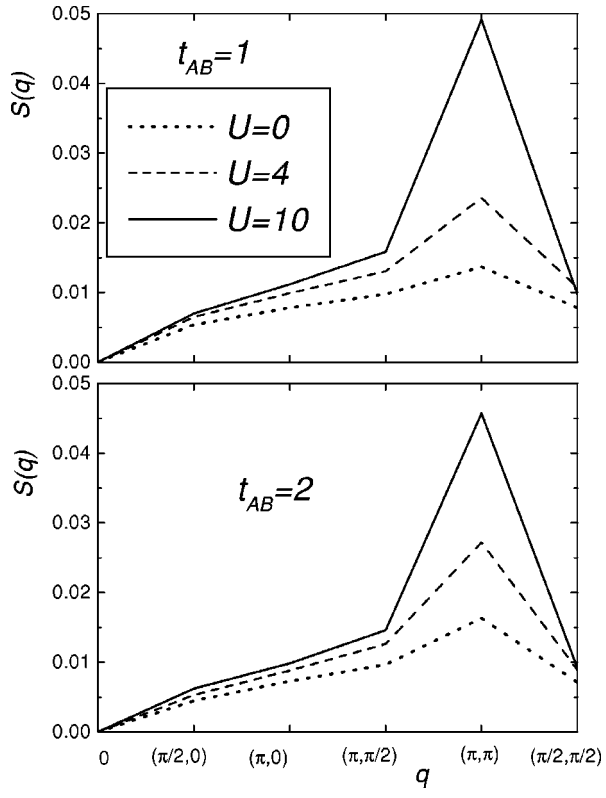

FIG. 2. Spin-structure factor as a function of wave vector for $N=14$ and different values of t_{AB} and U.

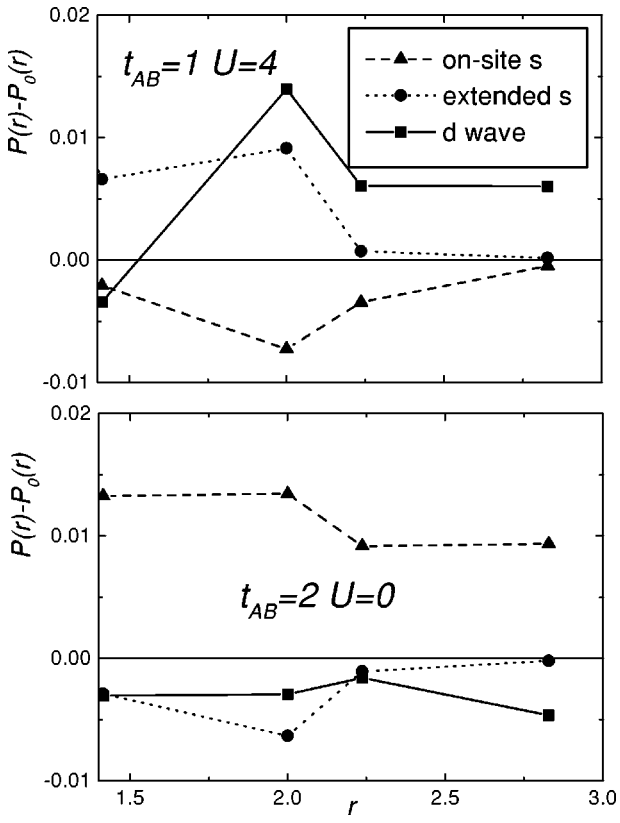

FIG. 3. $\overline{P}_\alpha(r)$ for $N=12$ and different parameters ($t_{AB}=1$, $U=4$; $t_{AB}=2$, $U=0$).

We have also calculated charge and spin correlation functions. The spin-structure factor is

$$S(\mathbf{q})=\sum_{ij}\langle S_i^z S_j^z \exp[i\mathbf{q}\cdot(\mathbf{R}_i-\mathbf{R}_j)]\rangle/L^2, \tag{3}$$

with $L=16$, and it indicates when one can expect a competition of superconductivity with antiferromagnetism.

In Fig. 1 we show the result of the different $P_\alpha(r)$ and $\overline{P}_\alpha(r)$ as functions of the distance r for $N=14$ (doping $x=0.125$) in the noninteracting case and for $t_{AB}=2$, $U=4$. The latter is the most significant set of values of t_{AB} and U for which some increase in one of the pairing correlation functions relative to the noninteracting case ($t_{AB}=1$, $U=0$) is observed. This $P_\alpha(r)$ corresponds to $d_{x^2-y^2}$-wave symmetry and $P_d(r)$ increases particularly at the largest distances within the cluster. The OBC correspond to MBC for $U\leqslant 4$ and PBC for $U=10$. For the noninteracting case, $\overline{P}_\alpha(r)$ should be zero in the thermodynamic limit, or for

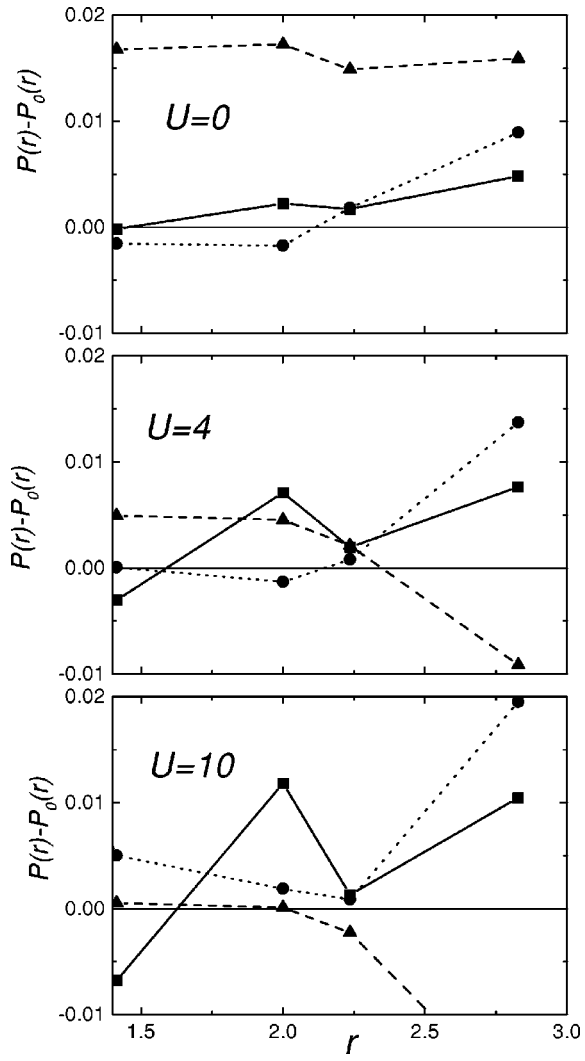

FIG. 4. $\overline{P}_{\alpha}(r)$ for $N=10$, $t_{AB}=2$ and three values of U. The meaning of the different symbols is the same as in Fig. 1.

finite size if the ground state is given by one Slater determinant. The latter is the case for all other dopings studied here. However, for $N=14$, the ground state is degenerate. As a consequence, for general values of t_{AB} and U, $\overline{P}_{\alpha}(r)$ should be compared with the result for $t_{AB}=1$, $U=0$ to extract conclusions regarding superconductivity. This comparison shows also a significant increase in $\overline{P}_{d}(r)$ for $t_{AB}=2$, at a moderate value $U=4$. For $t_{AB}=2$ and $U=0$, there is an increase of $P_{os}(r)$ and $\overline{P}_{os}(r)$ with respect to the noninteracting case (not shown). For $N=14$ and other parameters different from the above mentioned but within the region we have explored, there are no signals of superconductivity.

In Fig. 2 we show $S(\mathbf{q})$ for $N=14$ and different values of t_{AB} and U. In all cases, there is a rather sharp peak at wave vector (π,π). For $U\leqslant 4$, this peak increases slightly when t_{AB} is changed from 1 to 2. From the results in a finite system, we do not know if this peak evolves into a δ function with increasing system size, indicating an antiferromagnetic normal ground state, or into a broad peak indicating short-range antiferromagnetic correlations but allowing for

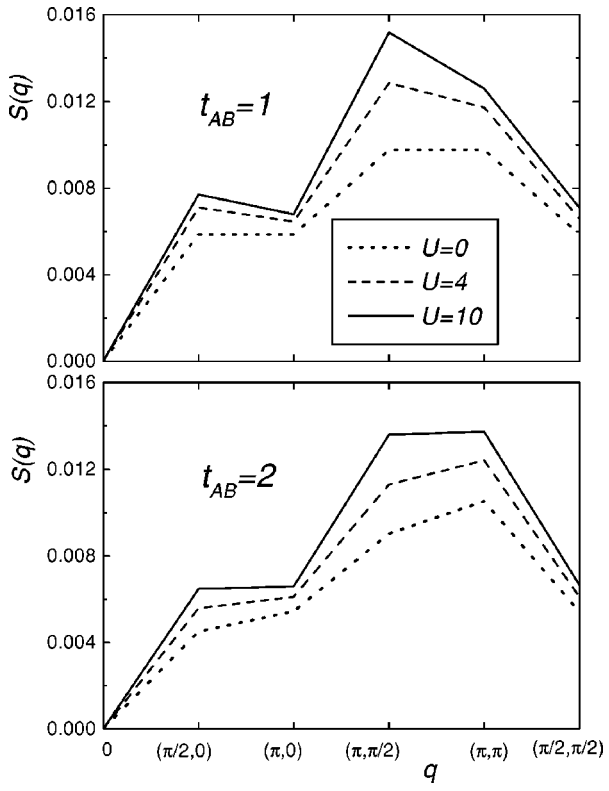

FIG. 5. Spin structure factor as a function of wave vector for $N=10$ and different values of t_{AB} and U.

$d_{x^2-y^2}$-wave superconductivity. The latter possibility was found in previous studies of hole-doped systems, such as those indicating a resonance-valence-bond wave function in the ground state[8] as well as in our previous analytical treatment of the present model including antiferromagnetic spin fluctuations.[26] In any case, our results suggest that the expected symmetry of the superconducting order parameter is x^2-y^2 for low electron doping.

For $N=12$, the OBC are MBC for all parameters studied. In the noninteracting case the ground state is nondegenerate and then all $\overline{P}_{\alpha}(r)=0$. In Fig. 3 we show the $\overline{P}_{\alpha}(r)$ for two sets of parameters where signals of superconductivity are obtained [similar conclusions can be reached comparing the $P_{\alpha}(r)$ with the noninteracting case]. For the Hubbard model including next-nearest-neighbor hopping with $U=4$ or $U=10$ (not shown), weak $d_{x^2-y^2}$-wave correlations seem to persist at large distances. The effect of increasing t_{AB} seems to reduce this pairing, although it persists for $t_{AB}=2$ and $U=10$. However, the small value of $\overline{P}_{d}(r)$ at large distances compared with its oscillations and the fact that for $N=14$ or for small hole doping,[26,27] t_{AB} helps rather than inhibits $d_{x^2-y^2}$-wave superconductivity, suggest that these results might be the consequence of finite-size effects. As before, s-wave superconductivity (of the on-site type) exists only for very small U.

For $N=10$, the OBC are PBC for all parameters. The $P_{\alpha}(r)$ for $d_{x^2-y^2}$-wave and extended s symmetry (not shown) have a marked zigzag structure (with maxima at $r=2$ and $r=2\sqrt{2}$) that seems to affect the vertex contribu-

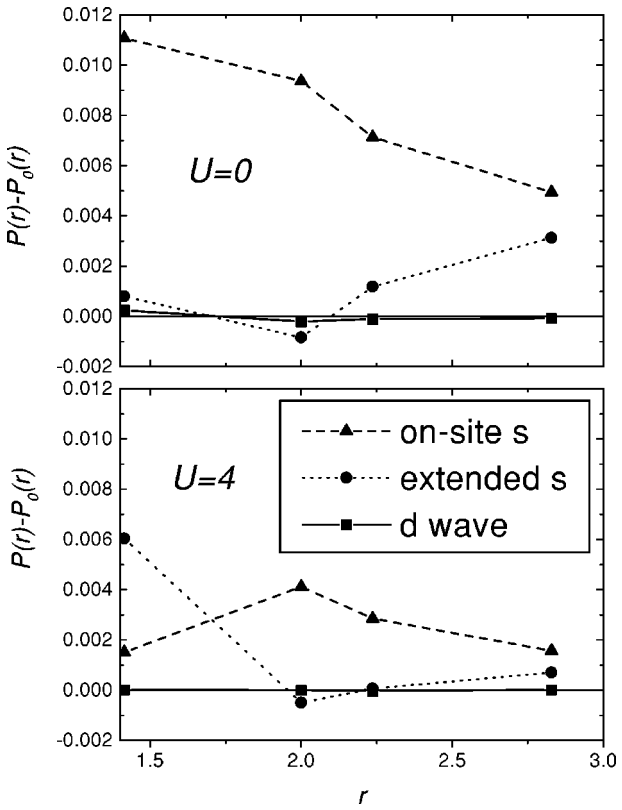

FIG. 6. $\overline{P}_\alpha(r)$ for $N=8$, $t_{AB}=2$ and two values of U.

tions $\overline{P}_\alpha(r)$ for large U. In any case, $P_d(r)$ is always smaller than in the noninteracting case. Concerning the $\overline{P}_\alpha(r)$, as shown in Fig. 4, one sees an increase in $\overline{P}_{os}(r)$ for $t_{AB}=2$ and $U=0$, as for the dopings previously considered, and some signals of extended s superconductivity, which might be due to finite-size effects, related with the above-mentioned zigzag structure. Nevertheless, there is an increase in $P_{es}(2\sqrt{2})$ in comparison with the noninteracting case.

The spin-structure factor has evolved with doping. As shown in Fig. 5, $S(\mathbf{q})$ is flatter and the main peak at (π,π) is displaced to incommensurate positions [near $(\pi,\pi/2)$] for small t_{AB}. This is somewhat similar to the shifts calculated in the hole-doped case.[27] However, for the same abolute value of the doping, the shifts are more pronounced in the hole-doped case.

For $N=8$, the OBC are ABC. The magnitude of $P_\alpha(r)$ and $\overline{P}_\alpha(r)$ is reduced as compared with previous cases. However, the $P_\alpha(r)$ are flatter and the results seem to be less affected by finite-size effects. For example, in the noninteracting case all $P_\alpha(r)<10^{-3}$ for $r\geq 2$. Then, we believe that our results are reliable. In agreement with previous expectations,[25] the vertex corrections shown in Fig. 6 suggest s-wave superconductivity with both on-site and extended s components for $t_{AB}=2$ and $U\leq 4$.

IV. SUMMARY AND DISCUSSION

Using exact diagonalization of a 4×4 cluster, we have studied the pairing correlation functions in the electron-doped Hubbard model with correlated hopping, derived before as an effective model for the cuprates. In comparison with the case of hole doping,[27] the analysis of the numerical results is more difficult due to the fact that the superconducting signals are smaller. In fact as explained in Sec. II, the vertex contributions $\overline{P}_\alpha(r)$ are expected to be proportional to the square of the superconducting order parameter, and the experimental fact that T_c is smaller in electron-doped cuprates, seems to be reflected in the calculations. Some experimental studies are also affected by this fact.[6]

From previous calculations using a generalized Hartree-Fock BCS decoupling, we expected to obtain s-wave superconductivity in the model.[25] Instead, clearly, for small doping the $d_{x^2-y^2}$-wave symmetry is preferred for realistic U. This suggests that at least near half filling, a Hartree-Fock decoupling of the on-site Coulomb repulsion U is inadequate for large U. A more realistic analytic description might be obtained in the nearly antiferromagnetic Fermi-liquid scenario.[26] On-site superconductivity takes place for very small values of U, and only for doping $x\gtrsim 0.37$ signals of s-wave superconductivity are obtained for moderate values of U.

As expected, the model is able to provide a nonconventional pairing mechanism of s-wave symmetry, without explicit attractive terms in the Hamiltonian. However, for the parameters more realistic for the cuprates, it seems that only $d_{x^2-y^2}$-wave pairing correlations show a significant enhancement with respect to the noninteracting case.

ACKNOWLEDGMENTS

L.A acknowledges support from CONICET. A.A.A. was partially supported by CONICET. This work was sponsored by PICT 03-06343 from ANPCyT and PIP 4952/96 of CONICET.

APPENDIX GENERALIZED *T-J* MODEL FOR ELECTRON-DOPED CUPRATES

Here we describe the derivation of an effective Hamiltonian for electron-doped cuprates in which the states with two holes at any site are integrated out of the relevant Hilbert space. The starting point is the three-band Hubbard model;[28]

$$H_{3b}=H_0+H_1+H_2,$$

$$H_0=\epsilon_d\sum_{i\sigma} n_{i\sigma}+\epsilon_p\sum_{j\sigma} n_{j\sigma}+U_d\sum_i n_{i\uparrow}n_{i\downarrow}+U_p\sum_j n_{j\uparrow}n_{j\downarrow}$$
$$+U_{pd}\sum_{i\delta\sigma\sigma'} n_{i\sigma}n_{i+\delta\sigma'}+\frac{U_{pp}}{2}\sum_{j\gamma\sigma\sigma'} n_{j\sigma}n_{j+\gamma\sigma'}, \quad \text{(A1)}$$

$$H_1=t_{pd}\sum_{i\delta\sigma}(p^\dagger_{i+\delta\sigma}d_{i\sigma}+\text{H.c.}), \quad H_2=-t_{pp}\sum_{j\gamma\sigma} p^+_{j+\gamma\sigma}p_{j\sigma}.$$

Here $d^{\dagger}_{i\sigma}$ creates a hole in the $3d_{x^2-y^2}$ orbital of Cu at site i. Similarly $p^{\dagger}_{j\sigma}$ creates a hole in the $2p$ orbital of O aligned along its two nearest-neighbor Cu atoms (usually called $2p_{\sigma}$ orbital), at site j. The operator $n_{i\sigma}=d^{\dagger}_{i\sigma}d_{i\sigma}$ and if the subscript is j, $i+\delta$, or $j+\gamma$ then $n_{j\sigma}=p^{\dagger}_{j\sigma}p_{j\sigma}$, etc. The four O atoms nearest neighbors to Cu site i (O site j) are denoted as $i+\delta$ $(j+\gamma)$.

In the case in which $U_d \gg t_{pd}$ and also the charge-transfer energy difference $\Delta=\epsilon_p-\epsilon_d \gg t_{pd}$, one can start from the (degenerate) ground state of H_0 and eliminate H_1 through a canonical transformation.[13] We must warn, however, that $\Delta \gg t_{pd}$ is not well satisfied in electron-doped systems,[22] and in this case one expects that Eq. (1) is a more realistic effective Hamiltonian. Calculating $e^{S}(H_0+H_1)e^{-S}=H'$ and choosing S in such a way that H' does not contain terms linear in H_1, the resulting transformed Hamiltonian becomes

$$H'=-4N\frac{t_{pd}^2}{\Delta+U_{pd}}+\sum_i 4t_{pd}^2\left(\frac{2}{\Delta+U_{pd}}-\frac{1}{\Delta}\right)n_i + \sum_{i\delta} 2t_{pd}^2\left(\frac{1}{\Delta}-\frac{1}{\Delta+U_{pd}}\right)n_i n_{i+2\delta} - \frac{t_{pd}^2}{\Delta}\sum_{i\delta\sigma} d^{\dagger}_{i+2\delta\sigma}d_{i\sigma}. \quad \text{(A2)}$$

Here, N is the number of unit cells. The first and second terms are trivial. The third term is an effective nearest-neighbor Cu-Cu repulsion driven by the original Cu-O repulsion and the last term is the nearest-neighbor Cu-Cu hopping, usual in the t-J model.

To transform H_2, one can use the result of the canonical transformation on $p_{j\sigma}$. After a simple algebra one obtains

$$e^{S}p_{j\sigma}e^{-S}=-{\sum_i}' (1-n_i)\frac{t_{pd}}{\Delta+U_{pd}{\sum_i}' n_i}d_{i\sigma}, \quad \text{(A3)}$$

where the sum runs over the two nearest-neighbor Cu atoms to O site j. Using Eq. (A3), the transformation of H_2 takes the form

$$e^{S}H_2e^{-S}=\frac{t_{pp}t_{pd}^2U_{pd}}{\Delta^2(\Delta+U_{pd})}\Bigg[4\sum_{i\delta} n_i n_{i+2\delta} - \frac{U_{pd}}{(\Delta+U_{pd})}\sum_{i\delta\perp\delta'} n_i n_{i+2\delta}n_{i+2\delta'} + 2\sum_{i\delta\perp\delta'\sigma} d^{\dagger}_{i+2\delta\sigma}d_{i\sigma}n_{i+2\delta'} + \left(2-\frac{U_{pd}}{\Delta+U_{pd}}\right)\sum_{i\delta\perp\delta'\sigma} n_i d^{\dagger}_{i+2\delta'\sigma}d_{i+2\delta\sigma}\Bigg] - 2\frac{t_{pp}t_{pd}^2}{\Delta^2}\left(2\sum_{i\delta\sigma} d^{\dagger}_{i+2\delta\sigma}d_{i\sigma}+\sum_{i\gamma\sigma} d^{\dagger}_{i+2\gamma\sigma}d_{i\sigma}\right). \quad \text{(A4)}$$

One of the most relevant terms here is the second one. It is a three-body attraction that favors to add the doped electrons in next-nearest-neighbor sites. This term is responsible for the attraction found in Ref. 16 using perturbation theory on states with $N-2$ static holes. However, to reach safe conclusions regarding superconductivity, the dynamics of the holes and realistic dopings have to be considered. The last term is a positive next-nearest-neighbor hopping t'.

Adding the usual superexchange term, the effective Hamiltonian is

$$H_{eff}=H'+e^{S}H_2e^{-S}+\frac{J}{2}\sum_{i\delta}\left(\mathbf{S}_i\cdot\mathbf{S}_{i+2\delta}-\frac{1}{4}\right), \quad \text{(A5)}$$

where $\mathbf{S}_i$ is the spin operator at Cu site i and up to order t_{pd}^4 and linear order in t_{pp},

$$J=\frac{4t_{pd}^4}{(\Delta+U_{pd})^2}\Bigg\{\frac{1}{U_d}\left(1+\frac{4t_{pp}}{\Delta+U_{pd}}+\frac{4t_{pp}}{\Delta+2U_{pd}}\right) + \frac{2}{2\Delta+U_p}\left[1+4t_{pp}\frac{4\Delta+3U_{pd}+U_{pp}}{(\Delta+U_{pd})(2\Delta+U_{pd}+U_{pp})}\right] + 8\frac{t_{pp}}{(2\Delta+U_{pd}+U_{pp})(\Delta+2U_{pd})}\Bigg\}. \quad \text{(A6)}$$

A numerical investigation of this model in a 4×4 cluster suggests that the three-body attraction in Eq. (A4) does not lead to increased pairing correlation functions of either s or $d_{x^2-y^2}$ symmetry. In fact, it favors phase separation.[18]

[1] Q. Huang, J.F. Zasadzinski, N. Tralshawala, K.E. Gray, D.G. Hinks, J.L. Peng, and R.L. Greene, Nature (London) **347**, 369 (1990).

[2] B. Stadlober, G. Krug, R. Nemetschek, R. Hackl, J.L. Cobb, and J.T. Markert, Phys. Rev. Lett. **74**, 4911 (1995).

[3] D.H. Wu, J. Mao, S.N. Mao, J.L. Peng, X.X. Xi, T. Venkatesan, R.L. Greene, and S.M. Anlage, Phys. Rev. Lett. **70**, 85 (1993).

[4] R. Prozorov, R.W. Giannetta, P. Fournier, and R.L. Greene, Phys. Rev. Lett. **85**, 3700 (2000).

[5] C.C. Tsuei and J.R. Kirtley, Phys. Rev. Lett. **85**, 182 (2000).

[6] N.P. Armitage, D.H. Lu, D.L. Feng, C. Kim, A. Damascelli, K.M. Shen, F. Ronning, Z.-X. Shen, Y. Onose, Y. Taguchi, and Y. Tokura, Phys. Rev. Lett. **86**, 1126 (2001).

[7] G. Kotliar, Phys. Rev. B **37**, 3664 (1988).

[8] C.D. Batista and A.A. Aligia, Physica C **264**, 319 (1996); C.D. Batista, L.O. Manuel, H.A. Ceccatto, and A.A. Aligia, Europhys. Lett. **38**, 147 (1997).

[9] J.F. Annett, N. Goldenfeld, and A.J. Leggett, J. Low Temp. Phys. **105**, 473 (1996).

[10] J. Nagamatsu, N. Nakagawa, T. Murakana, and J. Akimitsu, Nature (London) **410**, 63 (2001).

[11] Y. Kong, O.V. Dolgov, O. Jepsen, and O.K. Andersen, Phys. Rev.

B **64**, 020501(R) (2001); K. Voelker, V.I. Anisimov, and T.M. Rice, cond-mat/0103082 (unpublished).
[12] A.A. Abrikosov, Phys. Rev. B **52**, R15 738 (1995).
[13] C. Batista and A.A. Aligia, Phys. Rev. B **47**, 8929 (1993); A.A. Aligia, M.E. Simon, and C.D. Batista, *ibid.* **49**, 13 061 (1994).
[14] T. Tohyama and S. Maekawa, Phys. Rev. B **49**, 3596 (1994).
[15] G.A. Medina and M.D. Nuñez Regueiro, Phys. Rev. B **42**, 8073 (1990).
[16] J. Lorenzana and C.A. Balseiro, Phys. Rev. B **42**, 936 (1990).
[17] M.D. Núñez Regueiro and A.A. Aligia, Phys. Rev. Lett. **61**, 1889 (1988); J. Bala and A.M. Oleś, Phys. Rev. B **47**, 515 (1993); A.A. Aligia, M.D. Núñez Regueiro, and E.R. Gagliano, *ibid.* **40**, 4405 (1989); A.A. Aligia and M. Baliña, *ibid.* **47**, 14 380 (1993).
[18] S. Gómez, Master thesis, Instituto Balseiro, 1998.
[19] H.B. Schüttler and A.J. Fedro Phys. Rev. B **45**, 7588 (1992).
[20] M.E. Simon, M. Baliña, and A.A. Aligia, Physica C **206**, 297 (1993).
[21] M.E. Simon, A.A. Aligia, and E. Gagliano, Phys. Rev. B **56**, 5637 (1997), and references therein.
[22] Y. Ohta, T. Tohyama, and S. Maekawa, Phys. Rev. B **43**, 2968 (1991).
[23] E. Jeckelmann, D.J. Scalapino, and S.R. White, Phys. Rev. B **58**, 9492 (1998).
[24] S. Daul, D.J. Scalapino, and S.R. White, Phys. Rev. Lett. **84**, 4188 (2000).
[25] L. Arrachea and A. Aligia, Physica C **289**, 70 (1997).
[26] L. Arrachea and A. Aligia, Phys. Rev. B **59**, 1333 (1999).
[27] L. Arrachea and A. Aligia, Phys. Rev. B **61**, 9686 (2000).
[28] V.J. Emery, Phys. Rev. Lett. **58**, 2794 (1987); P.B. Littlewood, C.M. Varma, and E. Abrahams, *ibid.* **63**, 2602 (1989), and references therein.
[29] H. Chi and A.D.S. Nagi, Phys. Rev. B **46**, 421 (1992); M.J. Lercher and J.M. Wheatly, Physica C **215**, 145 (1993); R.J. Gooding, K.J.E. Vos, and P.W. Leung, Phys. Rev. B **49**, 4119 (1994); **50**, 12 866 (1994).
[30] E. Gagliano, E. Dagotto, A. Moreo, and F. Alcaraz, Phys. Rev. B **34**, 1677 (1986).
[31] G. Fano, F. Ortolani, and A. Parola, Phys. Rev. B **46**, 1048 (1992).
[32] L. Arrachea, A.A. Aligia, E. Gagliano, K. Hallberg, and C. Balseiro, Phys. Rev. B **50**, 16 044 (1994); **52**, 9793(E) (1995).
[33] L. Arrachea, Phys. Rev. B **62**, 10 033 (2000).
[34] S.R. White, D.J. Scalapino, R.L. Sugar, N.E. Bickers, and R.T. Scalettar, Phys. Rev. B **39**, 839 (1989).